Oligocatenanes Made to Order[1]

David B. Amabilino,[†,§] Peter R. Ashton,[†] Vincenzo Balzani,*[,#] Sue E. Boyd,[†] Alberto Credi,[#] Ju Young Lee,[†] Stephan Menzer,[‡] J. Fraser Stoddart,*[,†] Margherita Venturi,[#] and David J. Williams*[,‡]

Contribution from The School of Chemistry, The University of Birmingham, Edgbaston, Birmingham B15 2TT, UK, The Chemical Crystallography Laboratory, Department of Chemistry, Imperial College, South Kensington, London SW7 2AY, UK, and Dipartimento di Chimica "G. Ciamician" dell'Università, Via Selmi 2, 40126 Bologna, Italy

Received June 24, 1997. Revised Manuscript Received March 15, 1998

Abstract: The construction of catenanes, comprised of between two and seven interlocked rings, has been achieved. Two tris-1,5-naphtho-57-crown-15 macrocycles template the formation of cyclobis(paraquat-4,4′-biphenylene) to give a [3]catenane, which acts as a template for the construction of one and then another cyclobis(paraquat-*p*-phenylene) to give a [4]- and [5]catenane (Olympiadane). When high pressure was used in these templated syntheses, a [6]- and [7]catenane, as well as a [5]catenane that is topologically isomeric with Olympiadane, were also obtained. X-ray analyses of the [3]-, [5]-, and [7]catenanes reveal an optimum use of electrostatic, $\pi-\pi$ stacking, [C−H···π] interactions, and [C−H···O] hydrogen bonds in the organization of the component rings within the molecules. Noteworthy in the [7]catenane structure is the location of four of the PF_6^- anions within voids present in the 20^+ ion. Temperature-dependent ^{1}H NMR spectroscopic studies and electrochemical investigations have revealed the dynamic and redox behavior of these catenanes in solution.

Introduction

Catenanes[2,3] are becoming commonplace molecular compounds. Recently, template-direction[4] and self-assembly,[5] assisted by supramolecular interactions,[6] have allowed many topologically fascinating molecules to be constructed.[7] Higher catenanes have proven to be more elusive[8]—so much so that the construction of multiply interlocked chainlike molecules remains a challenge.[9] The preparation[10] of [3]catenates with copper(I) as a template has spawned catenates containing up to seven interlocked rings as illustrated by **1** in Figure 1, where $n = 3$. Furthermore, polycatenanes of type **2** in Figure 1 have been formed by polymerization of preformed bifunctional [2]-catenane monomers.[11] However, the controlled creation of polycatenanes of types **3** or **4** in Figure 1 has yet to be addressed.[12] Indeed, high molecular weight linear polycatenanes might be regarded as a "holy grail" in unnatural product synthesis.[13] One of the attractions of these exotic molecules is the potential materials properties that they may possess on account of their mechanically interlocked components.[14] Con-

* Correspondence should be addressed to Dr. J. F. Stoddart, Department of Chemistry and Biochemistry, University of California at Los Angeles, 405 Hilgard Avenue, Los Angeles CA90095. Tel: 310-206-7078. Fax: 310-206-1843. E-mail: stoddart@chem.ucla.edu.

† University of Birmingham.

‡ Imperial College.

Universitá di Bologna.

§ Current Address: Institut de Ciència de Materials de Barcelona (CSIC), Campus Universitari, 08193-Bellaterra, Spain.

(1) Molecular Meccano 30. For part 29, see; Ballardini, R.; Balzani, V.; Credi, A.; Gandolfi, M. T.; Marquis, D. J. F.; Pérez-García, L.; Stoddart, J. F. *Eur. J. Org. Chem.* **1998**, *81*, 1−89.

(2) For comprehensive reviews on catenanes, see: (a) Dietrich-Buchecker, C. O.; Sauvage, J.-P. *Chem. Rev.* **1987**, *87*, 795−810. (b) Amabilino, D. B.; Stoddart, J. F. *Chem. Rev.* **1995**, *95*, 2725−2828. (c) Jäger, R.; Vögtle, F. *Angew. Chem., Int. Ed. Engl.* **1997**, *36*, 930−944.

(3) For a recent communication on catenanes, see: Hamilton, D. G.; Feeder, N.; Prodi, L.; Teat, S. J.; Clegg, W.; Sanders, J. K. M. *J. Am. Chem. Soc*. **1998**, *120*, 1096−1097.

(4) (a) Anderson, S.; Anderson, H. L.; Sanders, J. K. M. *Acc. Chem. Res.* **1993**, *26*, 469−475. (b) Hoss, R.; Vögtle, F. *Angew. Chem., Int. Ed. Engl.* **1994**, *33*, 375−384.

(5) (a) Lawrence, D. S.; Jiang, T.; Levett, M. *Chem. Rev.* **1995**, *95*, 2229−2260. (b) Gillard, R. E.; Raymo, F. M.; Stoddart, J. F. *Chem. Eur. J.* **1997**, *3*, 1933−1940.

(6) Fyfe, M. C. T.; Stoddart, J. F. *Acc. Chem. Res.* **1997**, *30*, 393−401.

(7) See, for example: (a) Walba, D. M.; Zheng, Q. Y.; Schilling, K. *J. Am. Chem. Soc.* **1992**, *114*, 6259−6260. (b) Nierengarten, J.-F.; Dietrich-Buchecker, C. O.; Sauvage, J.-P. *New J. Chem.* **1996**, *20*, 685−693.

(8) For an example of higher catenanes based on metal-ion templated synthesis, see: Dietrich-Buchecker, C. O.; Frommberger, B.; Lüer, I.; Sauvage, J.-P.; Vögtle, F. *Angew. Chem., Int. Ed. Engl.* **1993**, *32*, 1434−1437.

(9) Amabilino, D. B.; Stoddart, J. F. *Pure Appl. Chem.* **1993**, *65*, 2351−2359.

(10) Bitsch, F.; Hegy, G.; Dietrich-Buchecker, C. O.; Leize, E.; Sauvage, J.-P.; van Dorsselaer, A. *New J. Chem.* **1994**, *18*, 801−807.

(11) (a) Geerts, Y.; Muscat, D.; Müllen, K. *Macromol. Chem. Phys.* **1995**, *196*, 3425−3435. (b) Menzer, S.; White, A. J. P.; Williams, D. J.; Belohradsky, M.; Hamers, C.; Raymo, F. M.; Shipway, A. N.; Stoddart, J. F. *Macromolecules* **1998**, *31*, 295−307.

(12) Some not so convincing reports on linear polycatenanes have appeared in the literature at a time when the analytical techniques available for characterizing these compounds were not so sophisticated. For a lead article, see: Karagounis, G.; Pandi-Agathokli, I.; Kontaraki, E. *IUPAC Colloid & Interface Sci. International Conf.* **1975**, *1*, 671−678.

(13) Stoddart, J. F. *Nature* **1988**, *334*, 10−11.

(14) Relatively poorly defined macromolecular systems that can be regarded as polycatenanes have been prepared. They show interesting properties when compared with their noninterlocked components. See, for example: (a) Millar, J. R. *J. Chem. Soc.* **1960**, 1311−1317. (b) Garrido, L.; Mark, J. E.; Clarson, S. J.; Semlyen, J. A. *Polym. Commun.* **1985**, *26*, 55−57. A number of crystalline solids contain interlocked rings which are formed in the process of crystallization. However, their superstructures do not persist in solution. For pertinent articles on related solids with references therein, see: (c) Ermer, O. *J. Am. Chem. Soc.* **1988**, *110*, 3747−3754. (d) Stumpf, H. O.; Ouahab, L.; Pei, Y.; Grandjean, D.; Kahn, O. *Science* **1993**, *261*, 447−449. (e) Fujita, M.; Ibukuro, F.; Yamaguchi, K.; Ogura, K. *J. Am. Chem. Soc.* **1995**, *117*, 7287−7288. (f) Abrahams, B. F.; Batten, S. R.; Hamit, H.; Hoskins, B. F.; Robson, R. *Chem. Commun.* **1996**, 1313−1314. (g) Hirsch, K. A.; Wilson, S. R.; Moore, J. S. *Chem. Eur. J.* **1997**, *3*, 765−771.

S0002-7863(97)02087-8 CCC: $15.00
Published on Web 04/28/1998

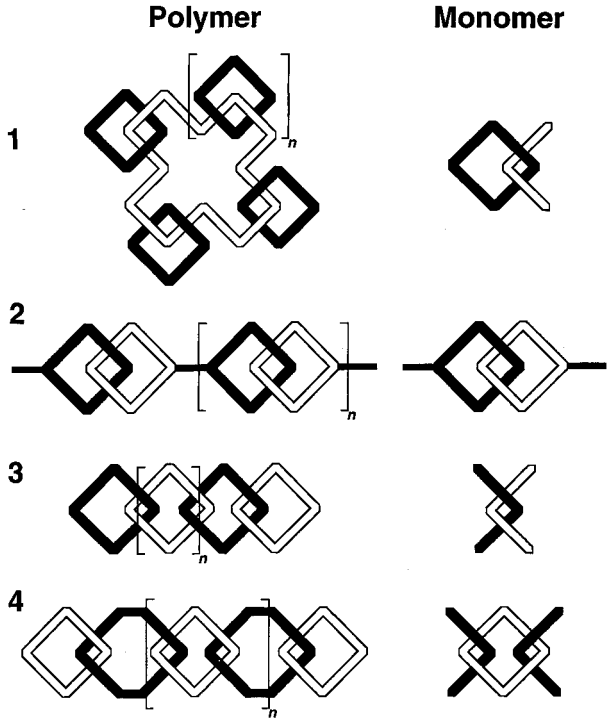

Figure 1. Cartoon representations of four types (**1**−**4**) of polycatenane.

sequently, we have embarked upon a "crusade" to fashion molecular chains. Our methodology exploits the cooperativity of weak noncovalent interactions—e.g. aromatic $\pi-\pi$ stacking,[15] [C−H···π] interactions,[16] and [C−H···O] hydrogen bonds[17]—between complementary components to construct interlocked molecules.[18] This approach has led to the self-assembly[5] of [2]-, [3]-, and bis[2]catenanes[19−21] and also to the linear [4]catenane,[22] **5**·8PF_6 in Figure 2. The subsequent progression to a compound believed to be a [5]catenane was highly inefficient, even under high-pressure reaction conditions.[23]

To improve the templating abilities of the previously employed macrocyclic polyether, tris-*p*-phenylene-51-crown-15 (**TPP51C15**), we replaced the three hydroquinone rings with 1,5-dioxynaphthalene ring systems[24] to give tris-1,5-naphtho-57-crown-15 (**TN57C15**). Here, we report the preparation of

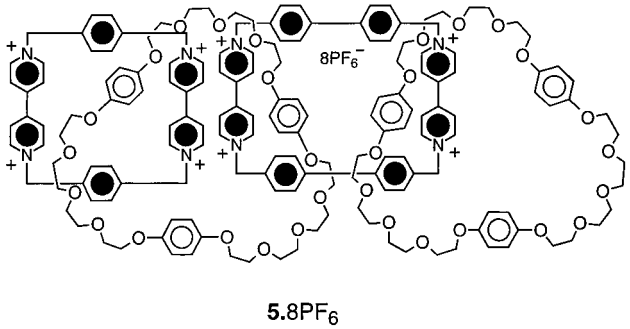

5.8PF_6

Figure 2. The [4]catenane **5**·8PF_6 which was formed from the macrocyclic polyether **TPP51C15** via the intermediate [3]catenane incorporating two macrocyclic polyethers and one cyclobis(paraquat-4,4′-biphenylene) tetracation.

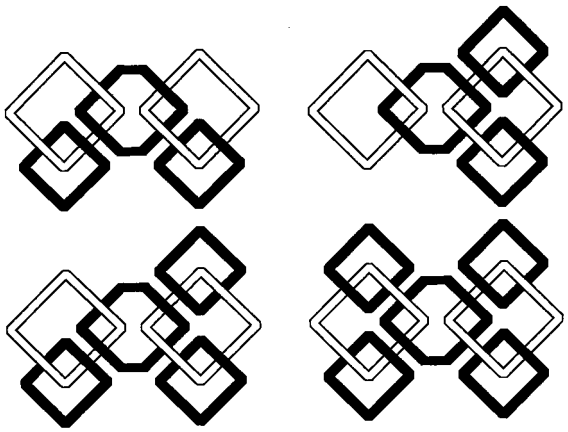

Figure 3. Cartoon representations of the two topologically stereoisomeric [5]catenanes, a [6]- and a [7]catenane.

TN57C15, as well as its ability to template the formation of cyclobis(paraquat-*p*-phenylene)[25] and cyclobis(paraquat-4,4′-biphenylene)[26] as integral components of catenanes. In particular, we describe the synthesis[27] of the linear pentacatenane, which we have named Olympiadane.[28] In addition, we have identified a topological stereoisomer[29] of Olympiadane, along with the intermediate [6]catenane, formed en route to a branched [7]catenane (Figure 3). The catenanes have been characterized by NMR spectroscopy, electrochemistry, and mass spectrometry. Highlights are the X-ray crystal structure of the heptacatenane[30] and of Olympiadane.[31]

(15) For reviews discussing $\pi-\pi$ stacking, see, along with references therein: (a) Dahl, T. *Acta Chem. Scand.* **1994**, *48*, 95−106. (b) Hunter, C. A. *Chem. Soc. Rev.* **1994**, 101−109. In the case of the types of compounds we are concerned with in this paper, the $\pi-\pi$ stacking leads to charge-transfer bands in the visible region of the electronic absorption spectrum. For a review concerning interactions between neutral donors and charged acceptors, see: Kamper, V. E. *Russ. Chem. Rev.* **1982**, *51*, 107−118. For a review on charge-transfer interactions in cyclophanes, see: Schwartz, M. H. *J. Inclusion Phenom.* **1990**, *9*, 1−35.

(16) Nishio, M.; Umezawa, Y.; Hirota, M.; Takeuchi, Y. *Tetrahedron* **1995**, *51*, 8665−8701.

(17) (a) Aekeröy, C. B.; Seddon, K. R. *Chem. Soc. Rev.* **1993**, *22*, 397−407. (b) Desiraju, G. R. *Chem. Commun.* **1997**, 1475−1482.

(18) Amabilino, D. B.; Stoddart, J. F.; Williams, D. J. *Chem. Mater.* **1994**, *6*, 1159−1167.

(19) Ashton, P. R.; Ballardini, R.; Balzani, V.; Credi, A.; Gandolfi, M. T.; Menzer, S.; Pérez-García, L.; Prodi, L.; Stoddart, J. F.; Venturi, M.; White, A. J. P.; Williams, D. J. *J. Am. Chem. Soc.* **1995**, *117*, 11171−11197.

(20) Ashton, P. R.; Brown, C. L.; Chrystal, E. J. T.; Goodnow, T. T.; Kaifer, A. E.; Parry, K. P.; Slawin, A. M. Z.; Spencer, N.; Stoddart, J. F.; Williams, D. J. *Angew. Chem., Int. Ed. Engl.* **1991**, *30*, 1039−1042.

(21) Ashton, P. R.; Huff, J.; Menzer, S.; Parsons, I. W.; Preece, J. A.; Stoddart, J. F.; Tolley, M. S.; White, A. J. P.; Williams, D. J. *Chem. Eur. J.* **1996**, *2*, 31−44.

(22) Amabilino, D. B.; Ashton, P. R.; Reder, A. S.; Spencer, N.; Stoddart, J. F. *Angew. Chem., Int. Ed. Engl.* **1994**, *33*, 433−437.

(23) Amabilino, D. B.; Ashton, P. R.; Brown, C. L.; Córdova, E.; Godínez, L.; Goodnow, T. T.; Kaifer, A. E.; Newton, S. P.; Pietraszkiewicz, M.; Philp, D.; Raymo, F. M.; Reder, A. S.; Rutland, M. T.; Slawin, A. M. Z.; Spencer, N.; Stoddart, J. F.; Williams, D. J. *J. Am. Chem. Soc.* **1995**, *117*, 1271−1293.

(24) The binding constants for substrates containing 1,5-dioxynaphthalene ring systems with—and consequently their templating actions in the formation of—cyclobis(paraquat-*p*-phenylene) are known to be greater than those for those substrates containing hydroquinone rings. See: Ashton, P. R.; Blower, M.; Philp, D.; Spencer, N.; Stoddart, J. F.; Tolley, M. S.; Ballardini, R.; Ciano, M.; Balzani, V.; Gandolfi, M. T.; Prodi, L.; McLean, C. H. *New J. Chem.* **1993**, *17*, 689.

(25) Asakawa, M.; Dehaen, W.; L'abbé, G.; Menzer, S.; Nouwen, J.; Raymo, F. M.; Stoddart, J. F.; Williams, D. J. *J. Org. Chem.* **1996**, *61*, 9591−9595.

(26) Asakawa, M.; Ashton, P. R.; Menzer, S.; Raymo, F. M.; Stoddart, J. F.; White, A. J. P.; Williams, D. J. *Chem. Eur. J.* **1996**, *2*, 877−893.

(27) Amabilino, D. B.; Ashton, P. R.; Reder, A. S.; Spencer, N.; Stoddart, J. F. *Angew. Chem., Int. Ed. Engl.* **1994**, *33*, 1286−1290.

(28) (a) Walba, D. M. *New J. Chem.* **1993**, *17*, 618. (b) van Gulick, N. *New J. Chem.* **1993**, *17*, 619−625..

(29) (a) Frisch, H. L.; Wasserman, E. *J. Am. Chem. Soc.* **1961**, *83*, 3789−3795. (b) Sokolov, V. I. *Russ. Chem. Rev.* **1973**, *42*, 452−463. (c) Walba, D. M. *Tetrahedron* **1985**, *41*, 3161−3212. (d) Chambron, J.-C.; Dietrich-Buchecker, C. O.; Sauvage, J.-P. *Top. Curr. Chem.* **1993**, *165*, 131−162.

Scheme 1

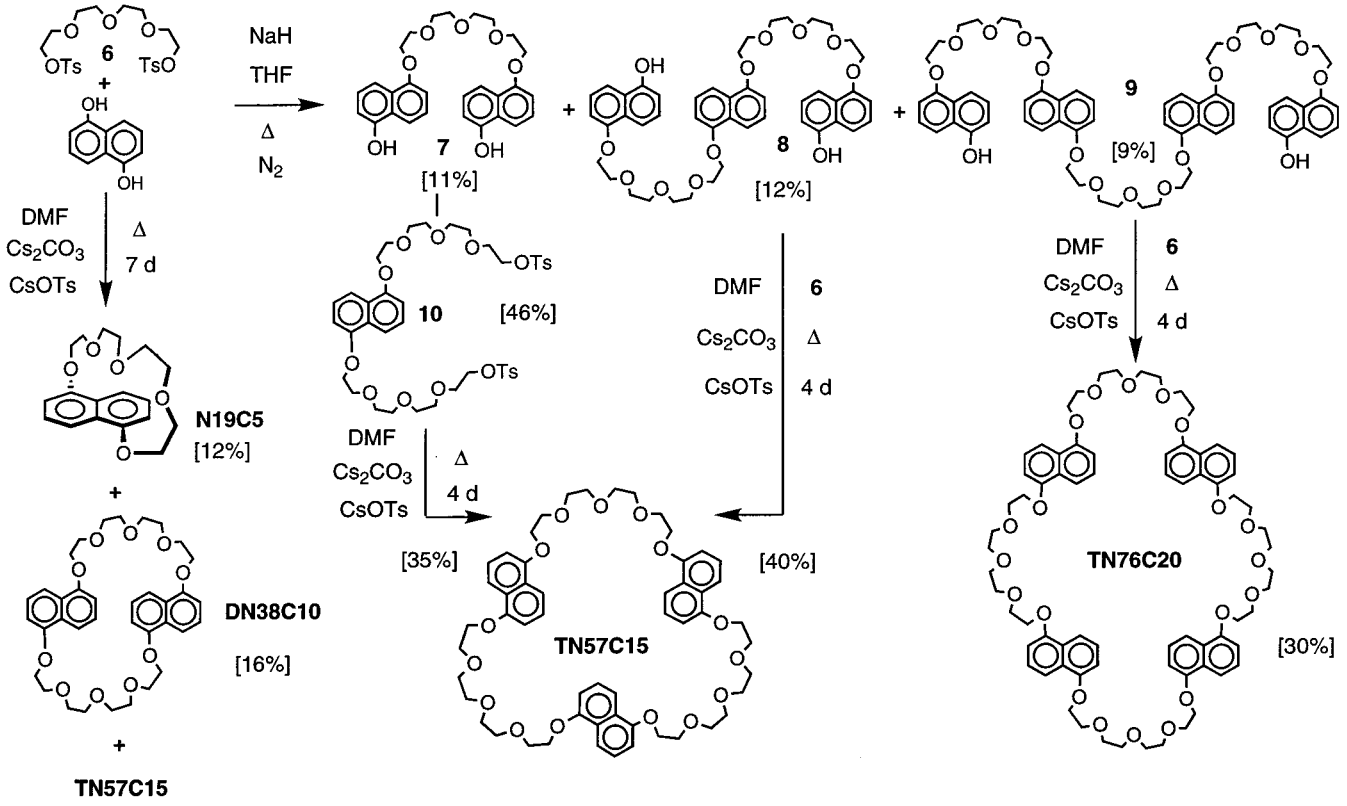

Results and Discussion

I. Synthesis of the Macrocyclic Polyethers. See Scheme 1. Reaction of **6** with 1,5-dihydroxynaphthalene, using Cs_2CO_3 as base,[32] afforded **TN57C15** along with 1,5-naphtho-19-crown-5 (**N19C5**) and di-1,5-naphtho-38-crown-10 (**DN38C10**).[33] On account of the low yield (6%) of **TN57C15**, an alternative preparation via the diols **7** and **8** was employed. Along with **DN38C10** (3%) and the diol **9**, **7**, and **8** were isolated when 1,5-dihydroxynaphthalene was treated with 1.0 mol equiv of NaH and 0.5 mol equiv of **6**. **TN57C15** was obtained by reacting **7** with **10** or **8** with **6**. The bistosylate **10** was prepared by reacting an excess of **6** with 1,5-dihydroxynaphthalene in DMF with K_2CO_3 as base. Finally, tetra-1,5-naphtho-76-crown-20 (**TN76C20**)[34] was obtained from reaction of **9** with **6**.

II. Self-Assembly of Catenanes Incorporating TN57C15. Reaction (Scheme 2) of **11**·$2PF_6$ with **12** in DMF in the presence of 0.5 mol equiv of **TN57C15** afforded, after chromatography and counterion exchange, the [2]- and [3]catenanes **13**·$4PF_6$ and **14**·$8PF_6$, respectively.[35] When the reaction was carried out at 12 kbar, the [4]catenane, in which the **TN57C15** ring is interlocked by three cyclobis(paraquat-*p*-phenylene) tetracations, has also been characterized. The efficiency of these template-directed processes compares favorably with the equivalent reactions[22] involving **TPP51C15** as the template where only the corresponding [2]catenane could be isolated.

The self-assembly of the [3]catenane **18**·$4PF_6$, incorporating cyclobis(paraquat-4,4′-biphenylene), was achieved by reaction (Scheme 3) of **15**·$2PF_6$ with **16** in MeCN/DMF (10:1) in the presence of an excess of **TN57C15**, followed by the "usual" workup procedure. A small amount of the [2]catenane[36] **17**·$4PF_6$ was also isolated. All attempts to increase the efficiency of this template-directed reaction were unsuccessful.[37] When **18**·$4PF_6$ was stirred with **11**·$2PF_6$ and **12** in DMF for 4 days, the [4]catenane **19**·$8PF_6$ and Olympiadane—the [5]catenane **20**·$12PF_6$—were obtained[27] in 31% and 5% yields, respectively, after the usual workup procedure. When the reaction time was extended to 14 days, these percentages rose to 51 and 18, respectively. Aside from unreacted [3]catenane, the reaction mixture also contained traces of higher catenanes.

The use of ultrahigh pressure[38] proved to be beneficial in promoting the cascade of self-assembly steps summarized in

(30) For a preview of the X-ray crystal structure of the heptacatenane, see: Amabilino, D. B.; Ashton, P. R.; Boyd, S. E.; Lee, J. Y.; Menzer, S.; Stoddart, J. F.; Williams, D. J. *Angew. Chem., Int. Ed. Engl.* **1997**, *36*, 2070−2072.

(31) For a preliminary glimpse of the X-ray crystal structure of Olympiadane, see: Dagani, R. *Chem. Eng. News* **1996**, Sept. 2, 31.

(32) For a review discussing the "cesium effect" upon cyclizations, see: Ostrowicki, A.; Koepp, E.; Vögtle, F. *Top. Curr. Chem.* **1991**, *161*, 37−67.

(33) Ashton, P. R.; Chrystal, E. J. T.; Mathias, J. P.; Parry, K. P.; Slawin, A. M. Z.; Spencer, N.; Stoddart, J. F.; Williams, D. J. *Tetrahedron Lett.* **1987**, *28*, 6367−6370.

(34) This macrocyclic polyether (**TN76C20**) can be used as a template for the formation of cyclobis(paraquat-*p*-phenylene), leading to a variety of catenanes, which will be described elsewhere by: Amabilino, D. B.; Lee, J. Y.; Stoddart, J. F. Unpublished results.

(35) Amabilino, D. B.; Ashton, P. R.; Stoddart, J. F.; Menzer, S.; Williams, D. J. *J. Chem. Soc., Chem. Commun.* **1994**, 2475−2478.

(36) In principle, this [2]catenane can act as a ditopic receptor for molecules incorporating π-electron rich and deficient moieties. See: Amabilino, D. B.; Stoddart, J. F. *Supramolecular Stereochemistry*; Siegel, J. S., Ed.; Kluwer: Boston, 1995; pp 33−40. Preliminary experiments indicate that the [2]catenane **17**·$4PF_6$ does indeed act as a host for 1,5-dioxynaphthalene derivatives: Amabilino, D. B.; Stoddart, J. F. Unpublished results.

(37) The highest yield achieved for a catenation involving this tetracationic cyclophane is 31%. It has been attained by using the macrocyclic polyether **DN38C10** as a the template. The selectivity displayed for the formation of the [3]catenane in preference to the [2]catenane in the self-assembly process is less for **TN57C15** than for **DN38C10**. A similar phenomenon was observed for the hydroquinone ring-containing macrocyclic polyether templates.

(38) Isaacs, N. S. *Tetrahedron* **1991**, *47*, 8463−8497.

Scheme 2

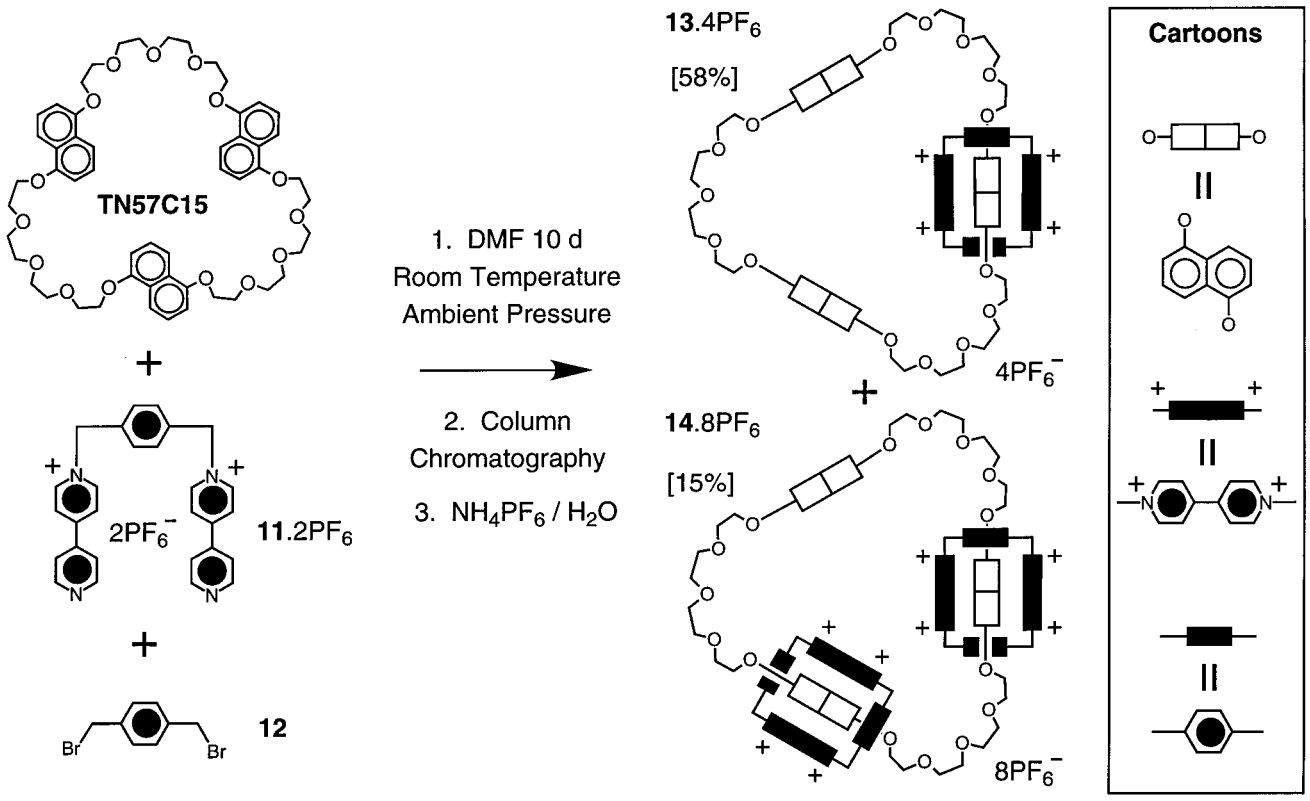

Scheme 3. After 6 days at 12 kbar of pressure, *none* of the [3]catenane **18**·4PF_6 was present in the reaction mixture, from which the [5]-, [6]-, and [7]catenanes **20**·12PF_6, **22**·16PF_6, and **23**·20PF_6 were isolated as the major products. In addition, traces of the topological stereoisomer[29] of **20**·12PF_6, namely the branched [5]catenane **21**·12PF_6, were present in the chromatography fractions containing Olympiadane. The two isomeric [5]catenanes can be separated by fractional crystallization (vapor diffusion of *i*-Pr_2O into EtOAc/MeCN solution) since **20**·12PF_6 forms deep purple needlelike crystals, whereas **21**·12PF_6 precipitates from solution subsequently as an amorphous powder. The self-assembly process favors greatly the formation of the linear pentacatenane in preference to its branched isomer. The [7]catenane **23**·20PF_6 results from the templated formation of cyclobis(paraquat-*p*-phenylene) tetracations around all four 1,5-dioxynaphthalene ring systems that are "free" in the [3]catenane **18**·4PF_6. When hydroquinone rings are present in the macrocyclic polyether components of the [3]catenane instead of 1,5-dioxynaphthalene ring systems, the major product isolated from an analogous reaction is a [4]catenane.[22] This observation reaffirms the fact that 1,5-dioxynaphthalene ring systems template the formation of cyclobis(paraquat-*p*-phenylene) tetracations far more efficiently than do hydroquinone rings.[39]

III. X-ray Crystal Structures. The X-ray of **18**·4PF_6 shows (Figures 4 and 5) the molecule to have C_i symmetry with four of the six 1,5-dioxynaphthalene ring systems (D) forming a DADDAD stack with two bipyridinium units (A). The extended $\pi-\pi$ stacking interactions within the [3]catenane are augmented by (i) [C−H···π] interactions as illustrated in Figure 4b and (ii) two [C−H···O] hydrogen bonds (see the caption for Figure 4). The [3]catenanes are packed to form extended two-dimensional mosaic-like sheets (Figure 6) cemented by further $\pi-\pi$ and [C−H···π] interactions.

The solid-state structure of **20**·12PF_6 shows (Figures 7 and 8) the molecule to have maximized its potential for $\pi-\pi$ stacking between the components. These interactions are accompanied by the series of [C−H···π] interactions illustrated in Figure 7 and also [C−H···O] hydrogen bonds (see the caption for Figure 7). Despite the absence of any intermolecular $\pi-\pi$ stacking interactions involving the smaller tetracationic cyclophanes, the [5]catenane molecules aggregate to form sheets that are essentially coplanar with the mean planes of these smaller cyclophanes. There are intersheet $\pi-\pi$ stacking interactions between one of the rings of each biphenylene unit (of the large tetracationic cyclophane) of lattice-translated molecules.

One of the tantalizing questions posed by the structure of the [5]catenane was the following: How can additional cyclobis(paraquat-*p*-phenylene) tetracations be clipped on to the "non-encircled" 1,5-dioxynaphthalene ring systems in $\mathbf{20}^{12+}$? The answer is provided by the X-ray structure (Figure 9) of the branched [7]catenane. Both **TN57C15** macrocycles are "opened out" to form pseudo-C_3 symmetric arrangements of their three 1,5-dioxynaphthalene ring systems. These "dilations" are sufficient to permit the accommodation of an additional encircling cyclobis(paraquat-*p*-phenylene) tetracation onto each macrocyclic polyether. We now have the optimum scenario in that all the π-electron rich and deficient moieties have been utilized in the self-assembly of the interlocked molecular compound **23**·20PF_6. The process of "dilating" each of the **TN57C15** macrocycles creates small voids at the centers of these rings, permitting the docking of pairs of PF_6^- anions (Figure 10) into both their upper and lower surfaces. The [C···F] contacts between both pyridinium and phenylene carbon atoms

(39) Although the ring-closure reaction in this catenation is controlled by kinetics, the thermodynamics of binding clearly must play an initial role in the self-assembly process. See: Amabilino, D. B.; Ashton, P. R.; Pérez-García, L.; Stoddart, J. F. *Angew. Chem., Int. Ed. Engl.* **1995**, *34*, 2378−2380.

Scheme 3

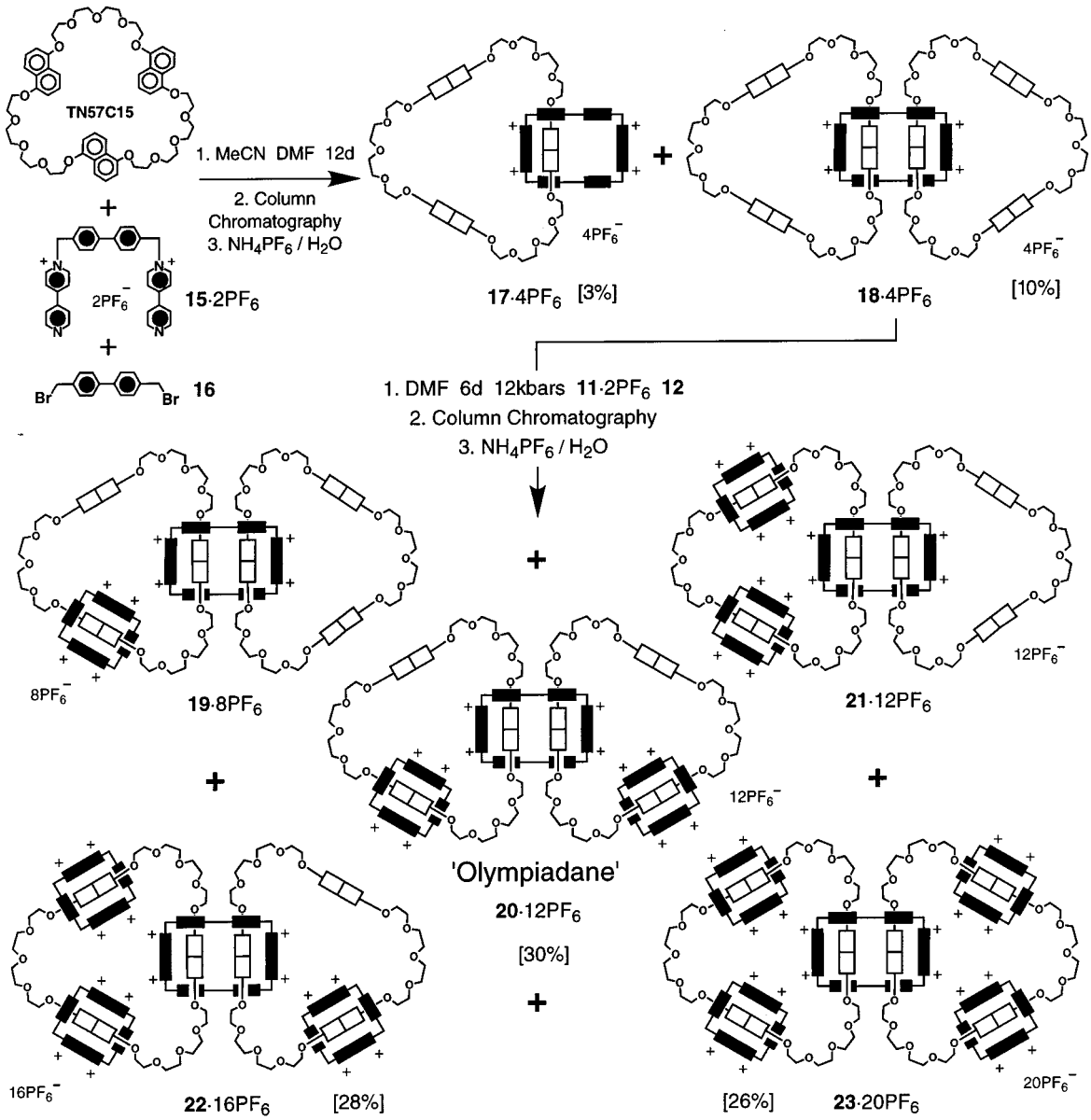

and the embedded anions indicate[40] that they are being held in position via a series of [C−H···F] hydrogen bonds. The [C···F] contacts are less than 3.2 Å and the orientations of the aryl rings provide favorable directionalities of their peripheral C−H bonds. Further support for the above conclusions comes from the fact that all four of these anions are ordered—a comparatively rare situation for PF_6^- anions.[41]

IV. Mass Spectrometry. FAB and LSI mass spectrometries were employed in the characterization of all the new catenanes. The general features of the spectra reveal signals resulting (i) from the loss of PF_6^- anions and then (ii) from the loss of the component macrocycles.[42] Both "fragmentation" patterns are typical[19] of these kinds of interlocked compounds. The LSI mass spectrum (Figure 11) of the [7]catenane (molecular formula, $C_{300}H_{300}N_{20}O_{30}P_{20}F_{120}$) reveals a clutch of peaks for the molecular ion with loss of between two and six PF_6^- anions. All of the observed peaks are based on the centroid of that expected for an unresolved isotopic distribution of atoms. Similar groups of signals are observed for the loss of cyclophanes from the heptacatenane, leading to signals corresponding to the [6]catenane **22**·16PF_6 and the [5]catenanes **20**·12PF_6 and **21**·12PF_6, and so on.

V. ^{1}H NMR Spectroscopy. The relevant ^{1}H NMR chemical shift data for the catenanes and their components—**TN57C15**, cyclobis(paraquat-*p*-phenylene) **24**$^{4+}$, and cyclobis(paraquat-4,4′-biphenylene) **25**$^{4+}$—are summarized in Table 1. The kinetic and thermodynamic data[43] associated with the relative movements of the catenane components are listed in Table 2.

In the catenanes **13**·4PF_6 and **14**·8PF_6, incorporating **TN57C15** and respectively one and two cyclobis(paraquat-*p*-phenylene)

(40) In view of the limited resolution of the data, we have not carried out a detailed analysis of potential [C−H···O] and [C−H···F] interactions, though these undoubtedly will be playing a supporting role in the cooperative forces that constitute the "adhesive" within this complex multicomponent molecule.

(41) Recently, however, we have uncovered, in a series of solid state structures, a significant number of highly ordered PF_6^- anions trapped within crystalline supermolecules made up of crown ethers as receptors for organic cations containing one or two secondary dialkylammonium centers. See for example: Fyfe, M. C. T.; Glink, P. T.; Menzer, S.; Stoddart, J. F.; White, A. J. P.; Williams, D. J. *Angew. Chem., Int. Ed. Engl.* **1997**, *36*, 2068−2070.

(42) The characteristics of the mass spectra of catenanes were first described by: Vetter, W.; Schill, G. *Tetrahedron* **1967**, *23*, 3079−3093.

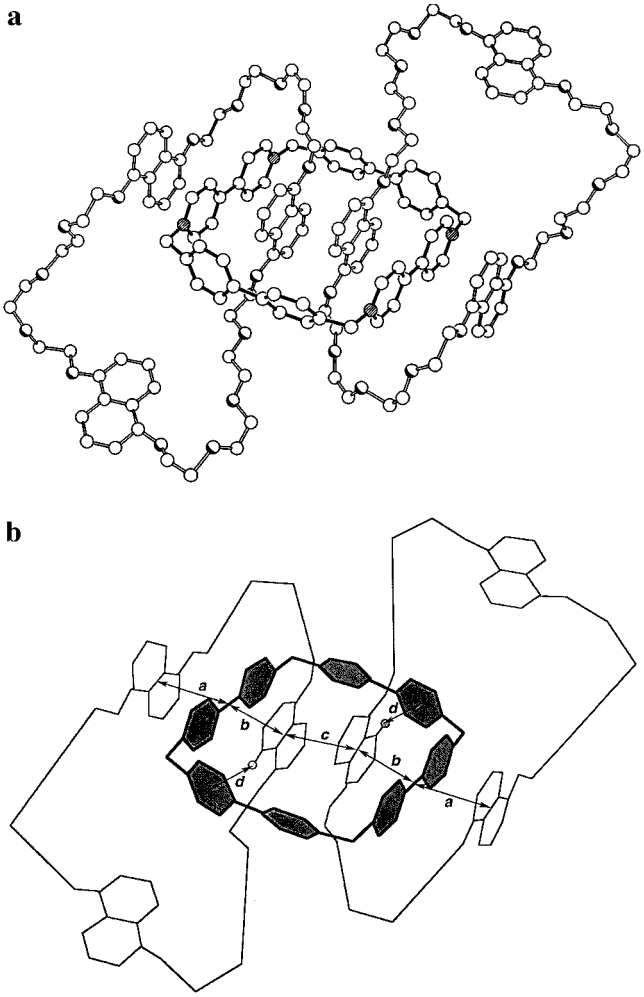

Figure 4. (a) Ball-and-stick representation of the [3]catenane $\mathbf{18}^{4+}$ (shaded circle = N, part shaded circle = O, open circle = C) and (b) a related cartoon version showing the aromatic $\pi-\pi$ stacking and edge-to-face [C−H···π] interactions: mean interplanar separation (Å) associated with $\pi-\pi$ stacking (***a*** 3.39; ***b*** 3.35; ***c*** 3.55 Å) and [H···π centroid] distance, [C−H···π] angle (***d*** 2.74 Å, 142°). The molecular structure is stabilized further by [C−H···O] hydrogen bonds involving α-bipyridinium protons at two centrosymmetrically related corners of the tetracationic cyclophane and the central crown ether oxygen atoms in the nearby polyether loops of the macrocyclic polyether component: [C···O] and [H···O] distances and [C−H···O] angle 3.16 Å, 2.26 Å, 157°.

tetracations, equilibration between the included and free 1,5-dioxynaphthalene residues is slow on the ^{1}H NMR time scale (400 MHz) at room temperature. This picture is supported by the fact that the hydrogen atoms—H-2/6, H-3/7, and H-4/8—on the naphthalene ring system included "inside" the tetracationic cyclophane resonate at approximately δ 6.1, 5.7, and 2.1, respectively. The signals from the H-4/8 hydrogen atoms appear at very high field because they are directed toward the π-face of the *p*-xylyl spacer of the cyclophane components in solution as in the solid state. The corresponding signals for the "outside" naphthalene ring systems resonate in the region of δ 6.5, 7.2, and 7.4, respectively. The mean chemical shifts (Table 1) for the α-CH and β-CH bipyridinium protons, as well as for the

(43) The kinetic and thermodynamic data were calculated by using the *coalescence method*, where values for the rate constant k_c at the coalescence temperature (T_c) were calculated (Sutherland, I. O. *Annu. Rep. NMR Spectrosc.* **1971**, *4*, 71−235) from the approximate expression $k_c = \pi(\Delta\nu)/(2)^{1/2}$, where $\Delta\nu$ is the chemical shift difference (in Hz) between the coalescing signals in the absence of exchange. The Eyring equation was subsequently employed to calculate $\Delta G^{\ddagger}_c$ values from k_c at T_c.

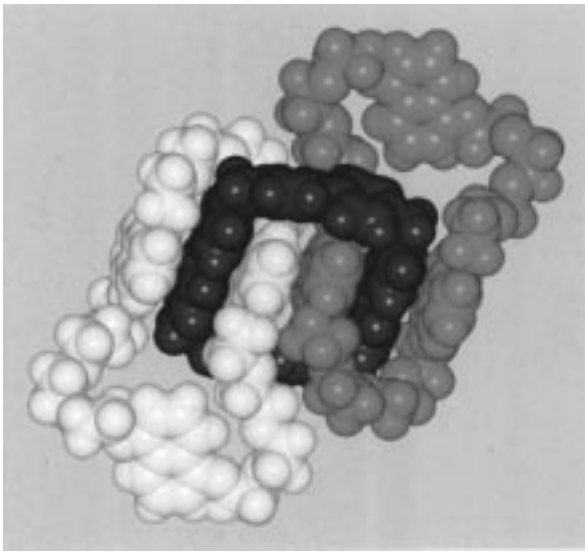

Figure 5. Space-filling representation of the [3]catenane $\mathbf{18}^{4+}$.

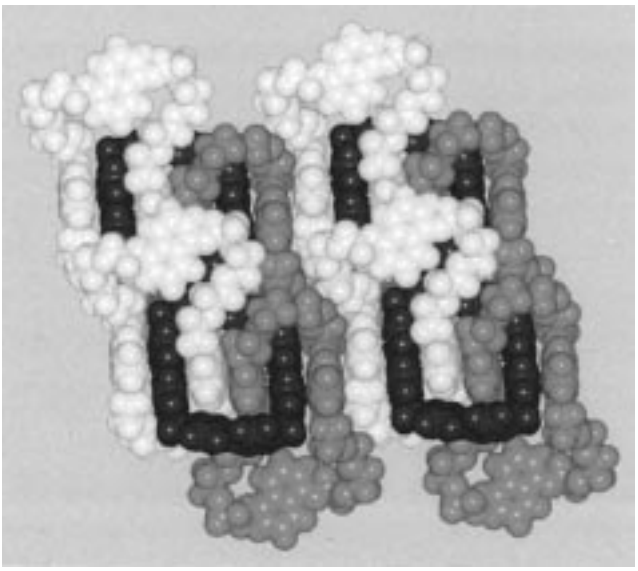

Figure 6. Space-filling representation of the crystal packing in [3]-catenane $\mathbf{18}^{4+}$.

protons on the phenylene ring in the cyclophanes, appear at increasingly lower fields as the number of cyclophanes is increased from one to two to three on the **TN57C15** macrocycle, an observation that is a result of the decreased "alongside" interaction of the 1,5-dioxynaphthalene ring systems with the bipyridinium units. The solid-state structure of $\mathbf{13}\cdot 4PF_6$ reveals $\pi-\pi$ stacking interactions of the "outside" 1,5-dioxynaphthalene ring systems with both a bipyridinium unit and one of the phenylene spacers in the cyclophane component—a situation that seems to be sustained, at least to some extent, in solution.[35] At just below 273 K, the ^{1}H NMR spectrum[44] of the [3]catenane $\mathbf{14}\cdot 8PF_6$ reveals a total of four resonances for the eight α-CH and eight β-CH protons associated with the bipyridinium units of the two cyclophanes. First, two α-CH proton environments are created by the local C_{2h} symmetry imposed on the cyclophanes by the included 1,5-dioxynaphthalene ring systems. Second, one side of each of the cyclophanes is directed toward each other whereas the other side, in each case, is pointing in the direction of the one unoccupied or "outside" 1,5-dioxynaph-

(44) The ^{1}H NMR spectra of the [3]catenane $\mathbf{14}\cdot 8PF_6$ were too complex to afford kinetic data.

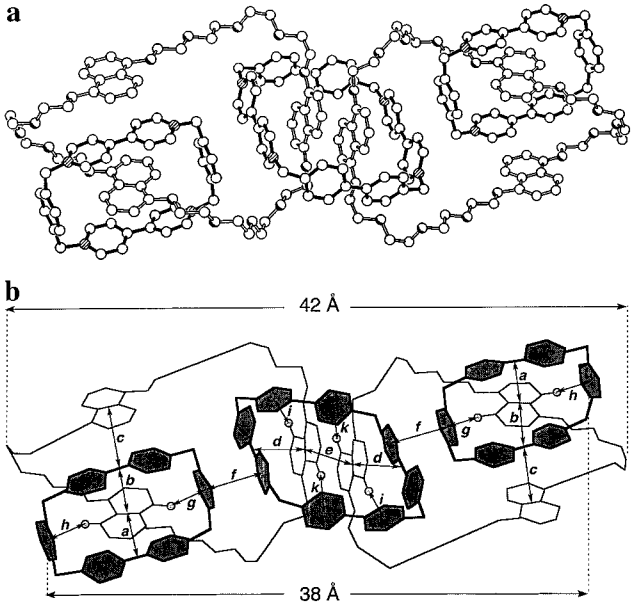

Figure 7. (a) Ball-and-stick representation of olympiadane $\mathbf{20}^{12+}$ (shaded circle = N, part shaded circle = O, open circle = C) and (b) a related cartoon version showing the aromatic $\pi-\pi$ stacking and edge-to-face [C−H···π] interactions: mean interplanar separation (Å) associated with $\pi-\pi$ stacking (***a*** 3.3; ***b*** 3.4; ***c*** 3.4; ***d*** 3.5; ***e*** 3.7; ***f*** 3.6 Å) and [H···π centroid] distance, [C−H···π] angle (***g*** 2.52 Å; 147°; ***h*** 2.63 Å, 147°; ***i*** 2.91 Å, 144°; ***k*** 2.88 Å, 160°). The twist angle of the large cyclophane with reference to the small one is 74°. The tilt angle of the large cyclophane with respect to the small one is ca. 25°. The molecular structure is stabilized further by [C−H···O] hydrogen bonds involving α-bipyridinium protons in the tetracationic cyclophanes and crown ether oxygen atoms in the two macrocyclic polyether components: [C···O] and [H···O] distances and [C−H···O] angle 3.18, 2.32 Å, 149° and 3.30, 2.41 Å, 153° involving the larger tetracation and 3.16, 2.29 Å, 152° and 3.25, 2.43 Å, 144° involving the smaller tetracation.

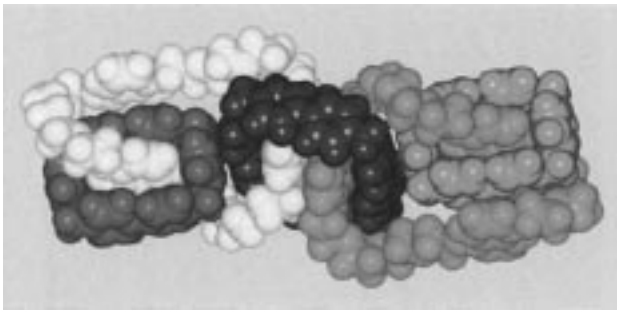

Figure 8. Space-filling representation of olympiadane $\mathbf{20}^{12+}$.

thalene residue. This sidedness is also evident and is expressed in the two signals observed for each of the constitutionally identical hydrogen atoms on the "inside" 1,5-dioxynaphthalene residues. The energy barrier for the coalescence behavior of the α-CH bipyridinium proton resonances in the [2]catenane $\mathbf{13}\cdot 4PF_6$ is recorded in Table 2. The exchange of the α-CH bipyridinium hydrogen atoms may result from one of two dynamic processes—by the 1,5-dioxynaphthalene residue departing from the cavity of the tetracationic cyclophane and then re-entering the cavity with a changed geometry or alternatively by the rotation of the bipyridinium unit about its long axis.[45]

The ^{1}H NMR chemical shift data for the catenanes $\mathbf{19}\cdot 8PF_6$, $\mathbf{20}\cdot 12PF_6$, $\mathbf{22}\cdot 16PF_6$, and $\mathbf{23}\cdot 20PF_6$ containing between four and seven rings, along with their "parent" [3]catenane $\mathbf{18}\cdot 4PF_6$, are listed in Table 1. Their partial ^{1}H NMR spectra at both 273 K and 343 K are compared in Figures 12 (parts a and b,

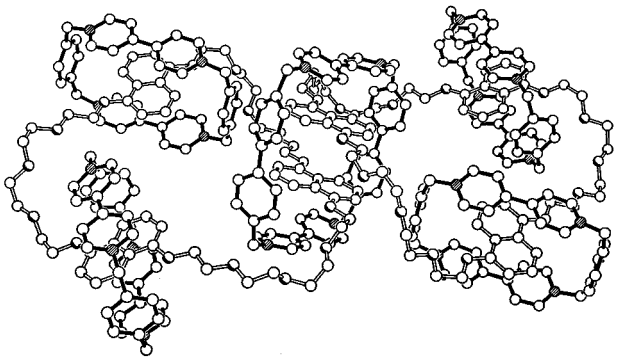

Figure 9. Ball-and-stick representation of the branched [7]catenane $\mathbf{23}^{20+}$ (shaded circle = N, part shaded circle = O, open circle = C) showing the alignment of each π-electron rich 1,5-dioxynaphthalene ring system with associated π-electron deficient bipyridinium units.

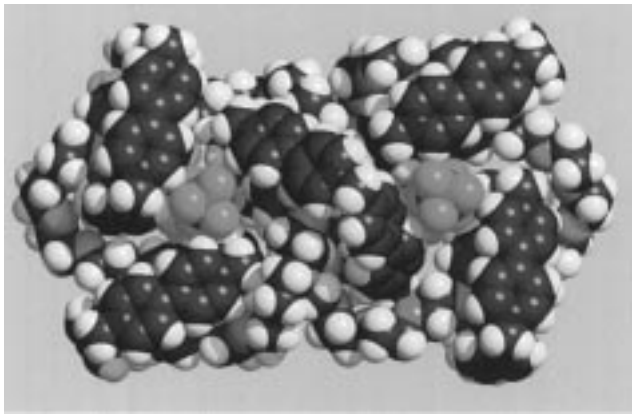

Figure 10. Space-filling representation of the branched [7]catenane $\mathbf{23}^{20+}$ showing the docked PF_6^- anions within the voids at the centers of each macrocyclic polyether ring. The front and back [P···P] separations are each 6.1 Å, and the associated side-to-side distances are 14.6 and 15.4 Å.

respectively). As the numbers of smaller tetracationic cyclophanes is increased on each of the macrocyclic polyether components, the resonances attributable to the α-CH and β-CH bipyridinium hydrogen atoms of the larger, central, tetracationic cyclophanes appear at increasingly low field. In the case of the less symmetrical [4]- and [6]catenanes, distinct resonances are observable for α-CH and β-CH protons of bipyridinium units residing in the nonequivalent polyether macrocycles.[46] Similarly, and perhaps more strikingly, the corresponding resonances of the smaller cyclophanes are influenced mainly by their immediate local environments, rather than by gross molecular structures. Two distinct sets of resonances are observed for the α-CH and β-CH bipyridinium hydrogen atoms of the smaller, peripheral, tetracationic cyclophanes, i.e., first, those whose immediate environment includes a **TN57C15** macrocycle with a single unoccupied recognition site (denoted by the symbol ⊙ in Figure 12), and second, tetracations located on macrocyclic

(45) (a) A similar process has been observed previously in a related [2]-catenane in which the same cyclophane and **DN38C10** are the two components. See: Ashton, P. R.; Brown, C. L.; Chrystal, E. J. T.; Goodnow, T. T.; Kaifer, A. E.; Parry, K. P.; Philp, D.; Slawin, A. M. Z.; Spencer, N.; Stoddart, J. F.; Williams, D. J. *J. Chem. Soc., Chem. Commun.* **1991**, 634−639. For a detailed kinetic analysis of the dynamic processes occurring in a related [3]catenane, see: (b) Ashton, P. R.; Boyd, S. E.; Claessens, C. G.; Gillard, R. E.; Menzer, S.; Stoddart, J. F.; Tolley, M. S.; White, A. J. P.; Williams, D. J. *Chem. Eur. J.* **1997**, *3*, 788−798.

(46) At 273 K, the resonances attributable to one set of α-CH and β-CH bipyridinium hydrogen atoms in the [4]catenane $\mathbf{19}\cdot 8PF_6$ are broadened by additional, unidentified, exchange processes. Resonances assignable to these nuclei are, however, resolved above room temperature as these processes enter the fast exchange regime (400 MHz).

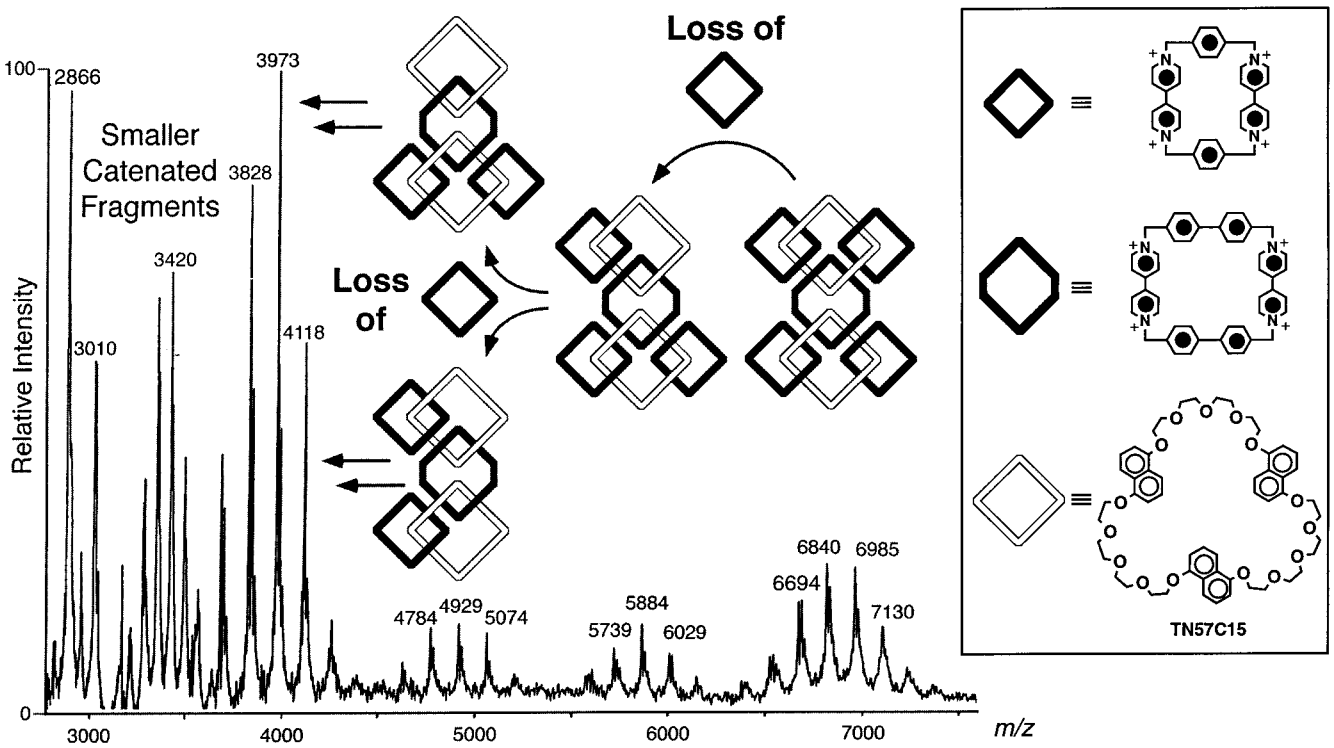

Figure 11. LSI mass spectrum of the [7]catenane **23**·20PF_6. Cartoons denote the groups of peaks attributable to the "fragment catenanes" arising from the successive loss of various component macrocycles. Within each group we see the sets of peaks attributable to the successive loss of PF_6^- anions from each of the "fragment catenanes".

Table 1. Selected ^{1}H NMR Data [δ Values in Ppm] in CD_3CN for the [*n*]Catenanes and Their Components

										naphthalene					
		small tetracationic cyclophane				large tetracationic cyclophane				"outside"			"inside"		
compound	*T*/K	αCH	*β*CH	C_6H_4	CH_2N^+	αCH	*β*CH	$(C_6H_4)_2$	CH_2N^+	H-2/6	H-3/7	H-4/8	H-2/6	H-3/7	H-4/8
TNP57C15	300									6.79	7.29	7.73			
24·4PF_6[a]	300	8.86	8.16	7.52	5.74										
25·4PF_6[a]	300					8.95	8.25	7.54	5.82						
								7.66							
13·4PF_6	273	8.32	6.79	7.59	5.48					6.56	7.18	7.44	5.97	5.68	2.11
		8.77	6.86	7.61	5.63					6.80	7.33	7.52			
14·8PF_6	268	8.36	7.86	7.65	5.39					6.38	7.00	7.00	6.10	5.77	2.05
		8.54	7.10	7.83	5.56								6.15	5.89	2.27
		8.68	7.10	7.90	5.66										
		9.04	7.11	7.98	5.72										
17·4PF_6	300					8.75	7.51	7.56	5.69	6.78[b]	6.51[b]	6.46[b]			
								7.64							
18·4PF_6	343					8.45	6.69	7.70	5.57	6.50[b]	6.63[b]	6.33[b]			
								7.93							
19·8PF_6	343	8.77	7.21	7.98	5.73	8.53	6.44	7.75	5.58	6.3−5.8[a]					
						8.57	6.87	7.90	5.76						
								8.00							
20·12PF_6	273	8.42	6.97	8.81	5.52	8.59	6.75	7.71	5.58	6.25−5.85[b]			6.10[c]	5.82[c]	2.10[c]
		8.84	7.07	8.85	5.59			7.95							
22·16PF_6	273	8.44[c]	6.99[c]	7.84[c]	5.55[c]	8.70	6.84	7.77	5.53	6.4−5.7[b]			5.44[e]	5.40[e]	2.20[c]
		8.64[d]	7.10[c]	7.88[c]	5.69[d]		6.96	7.81	5.59				6.13[c]	5.83[c]	2.30[d]
		8.86[c]	7.13[d]	7.94[d]				8.06					6.17[d]	5.92[d]	3.83[e]
		8.91[d]	7.31[d]	8.02[d]											
23·20PF_6	283	8.53	7.08	7.85	5.59	8.60	6.89	7.74	5.43				5.37[d]	5.37[d]	2.28[e]
		8.87	7.26	7.98				8.03					6.17[e]	5.88[d]	3.92[d]

[a] For the homologous [4]catenane, in which the **TN57C15** ring is interlocked by three cyclobis(paraquat-*p*-phenylene) tetracations, signals were observed at δ 8.56, 8.90 (αCH), δ 7.10, 7.29 (*β*CH), δ 7.89, 8.01 (C_6H_4), and δ 5.64 (CH_2N^+) for the tetracationic cyclophanes and at δ 6.17 (H-2/6), δ 5.91 (H-2/7), and δ 2.29 (H-4/8) for the "inside" naphthalene rings in a spectrum recorded in CD_3CN at 273 K. [b] Rings rotate through one another at such a rate that some of their associated resonances are broadened into the baseline of the NMR spectrum at this temperature. [c] Related to the small tetracation denoted by the symbol ⊙ in Figure 12. [d] Related to the small tetracations denoted by the symbol ● in Figure 12. [e] Related to the large tetracation.

polyethers in which all the recognition sites are occupied (denoted by the symbol ● in Figure 12). In the latter case, the absence of "alongside" interactions between free 1,5-dioxynaphthalene residues and the bipyridinium units of the small tetracations accounts most likely for the low field shift observed for these resonances relative to those of the former case.

Table 2. Kinetic and Thermodynamic Parameters Obtained from the Temperature-Dependent ^{1}H NMR Data Recorded for the [*n*]Catenanes[a]

compd	probe protons undergoing site-exchange	$\Delta\nu$ (Hz)	k_c (s^{-1})	T_c (K)	$\Delta G_c^{\ddagger}$ (kcal mol^{-1})
13·4PF_6[b]	α-CH {⊙}[d]	179	398	326	15.2
18·4PF_6[c]	α-CH {▼}[e]	210	467	204	9.3
19·8PF_6[b]	*β*-CH {⊙}[d]	44	98	297	14.7
	α-CH {▼}[e]	23	51	362	18.5
20·12PF_6[b]	α-CH {⊙}[d]	166	369	310	14.5
	β-CH {⊙}[d]	41	92	296	14.7
22·16PF_6[b]	*β*-CH {⊙}[d]	43	96	295	14.6
	β-CH {●}[f]	71	106	328	16.0
	β-CH {▼}[e]	48	158	327	16.2
23·20PF_6[b]	α-CH {●}[f]	136	302	337	16.0
	β-CH {●}[f]	74	165	327	15.9
	C_6H_4 {●}[f]	48	108	310	15.3

[a] Determined by the *coalescence method* (see ref 43 (v/v) CD_3CN/CD_3COCD_3). [d] Related to the small tetracation denoted by the symbol ⊙ in Figure 12. [e] Related to the large tetracation denoted by the symbol ▼ in Figure 12. [f] Related to the small tetracations denoted by the symbol ● in Figure 12.

The energy barriers obtained from the coalescence of the resonances for the α-CH and *β*-CH bipyridinium hydrogen atoms in the catenanes **18**·4PF_6, **19**·8PF_6, **20**·12PF_6, **22**·16PF_6, and **23**·20PF_6 are summarized in Table 2. The site-exchange rates, exhibited by the nuclei of the small tetracations, like their resonance frequencies, are influenced predominantly by their respective local environments. The site-exchange rates exhibited by the *β*-CH bipyridinium hydrogen atoms of tetracations, whose immediate environment includes a **TN57C15** macrocycle with a single unoccupied recognition site, are approximately 95 times per second at room temperature, whereas those, whose immediate environment includes a **TN57C15** macrocycle with no unoccupied recognition sites, approximate to 160 times per second at 328 K. The coalescence of the pairs of resonances observed for each of the α-CH and *β*-CH bipyridinium hydrogen atoms of the large tetracationic cyclophanes of the [4]- and [6]-catenanes provides a measure of the rate of circumrotation of the large tetracation through the cavities of the two macrocyclic polyether components, a dynamic process not observable in the more symmetrical systems. The rate of exchange of the *β*-CH protons in the [6]catenane is 106 times per second at 327 K, while for the α-CH protons of the linear [4]catenane, it is only some 50 times per second at 362 K. This large difference in the observed rate of the circumrotation of the large tetracation is attributed to "alongside" interactions of bipyridinium units with the unoccupied 1,5-dioxynaphthalene units of the two macrocyclic polyether components in **19**·8PF_6 (as witnessed in the crystal structure of the [3]catenane **18**·4PF_6) which are absent in **22**·16PF_6.

The quantification of the rates of circumrotation of the macrocyclic polyether components through the various tetracationic cyclophane components of the catenanes, **19**·4PF_6 to **23**·20PF_6, could not be achieved because of either the complexity of the spectra or the magnitudes of the energy barriers involved. Qualitative analysis of the spectra provided in Figures 12 and 13 shows that the site-exchange rates between the 1,5-dioxynaphthalene units vary markedly with the extent of the catenation of the molecules. In the [3]catenane **18**·4PF_6, the proton resonances of the *π*-electron rich units appear as well-resolved, averaged signals at 343 K, i.e., the exchange between free and included 1,5-dioxynaphthalene units is fast on the ^{1}H NMR time scale (400 MHz), while at 273 K they are broadened as a result of a slower exchange process being operative. It is also clear that the site-exchange rates involving 1,5-dioxynaphthalene protons decrease dramatically as the size of the catenanes increases. In the [7]catenane, an extremely highly ordered molecule in solution, the rate of movement of included 1,5-dioxynaphthalene residues between different recognition sites is slow on the ^{1}H NMR time scale, even at 343 K (Figure 13). The reason for the high activation energy of this process is clearly associated with the fact that it must involve the synchronous disruption of five *π*−*π* stacking interactions between *π*-electron rich moieties and *π*-electron deficient groups, in addition to numerous [C−H···O] hydrogen bonds, [C−H···*π*] T-type interactions, and other Coulombic interactions.

VI. Absorption Spectra. All the examined catenanes exhibit the well-known[19] charge-transfer bands in the visible region, which are not present in their isolated components. Since the energy and the intensity of a charge-transfer band depend on the precise nature of the interacting partners and on their distance in the present, very complicated systems specific assignments, such as those proposed for simpler catenanes,[47] cannot be made.

VII. Electrochemistry. A. Catenane Components. The three basic components of the oligocatenanes, namely the tetracationic cyclophanes **24**$^{4+}$ and **25**$^{4+}$ and the **TN57C15** macrocycle, contain electroactive units. The electrochemical data for all the examined compounds are gathered in Table 3.

The two bipyridinium units of **24**$^{4+}$ undergo a first simultaneous one-electron reduction at −0.28 V and a second one at −0.72 V.[19] The behavior of **25**$^{4+}$, where the two bipyridinium units are connected by biphenylene spacers, is very similar.

The **TN57C15** macrocycle contains three equivalent 1,5-dimethoxynaphthalene (**DMN**)-type electroactive units which undergo distinct oxidation processes.[48] Such a contrasting behavior between the tetracationic cyclophanes and **TN57C15** can be interpreted considering that, in the cyclophanes, the rigidity of the structure prevents interaction between the two bipyridinium units, whereas the flexible structure of the macrocycle allows the three **DMN**-type units to approach one another. The first oxidation process of **TN57C15** occurs at a potential (+0.98 V) much less positive than that of **DMN**. This result can be accounted for by the formation of a stabilized structure where the oxidized **DMN**-type unit is sandwiched between the two non-oxidized units. Upon further one-electron oxidation, the most stable structure could be one where the two oxidized units sandwich the non-oxidized one. After the third oxidation process, the three positively charged **DMN**-type units most likely separate.

On going from the separated cyclophane or macrocycle components to their catenanes, it can be expected that (i) electronic interactions between the donor units of macrocycle **TN57C15** and the acceptor units of cyclophanes **24**$^{4+}$ and **25**$^{4+}$ displace the reduction processes to more negative potentials and the oxidation processes to more positive potentials and (ii) the two bipyridinium units of each cyclophane and the three **DMN**-type units of the **TN57C15** macrocycle may maintain or lose their spatial equivalence; in the latter case, splitting of degenerate

(47) Ballardini, R.; Balzani, V.; Brown, C. L.; Credi, A.; Gillard, R. E.; Montalti, M.; Philp, D.; Stoddart, J. F.; Venturi, M.; White, A. J. P.; Williams, B. J.; Williams, D. J. *J. Am. Chem. Soc.* **1997**, *119*, 12503−12513.

(48) Two distinct oxidation processes have also been observed for the 1/5DN38C10 macrocyclic polyether, which contains two DMN-type units, see: Asakawa, M.; Ashton, P. R.; Balzani, V.; Credi, A.; Hamers, C.; Mattersteig, G.; Montalti, M.; Shipway, A. N.; Spencer, N.; Stoddart, J. F.; Tolley, M. S.; Venturi, M.; White, A. J. P.; Williams, D. J. *Angew. Chem., Int. Ed. Engl.* **1998**, *37*, 333−337.

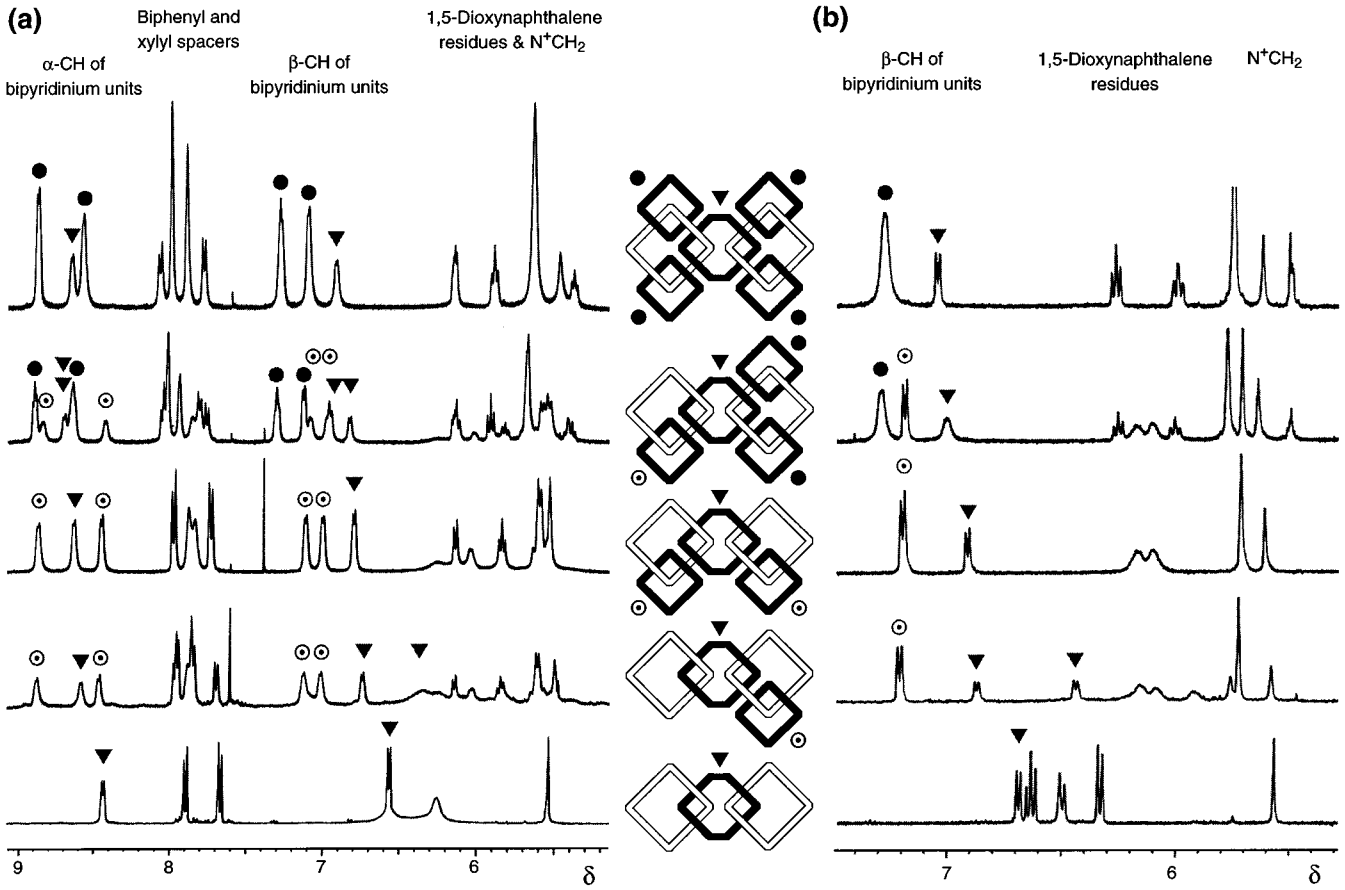

Figure 12. The partial ^{1}H NMR spectra of the catenanes, based on the parent [3]catenane **18**·4PF$_6$, containing between three and seven rings recorded at 400 MHz in CD_3CN at (a) 273 K and (b) 343 K.

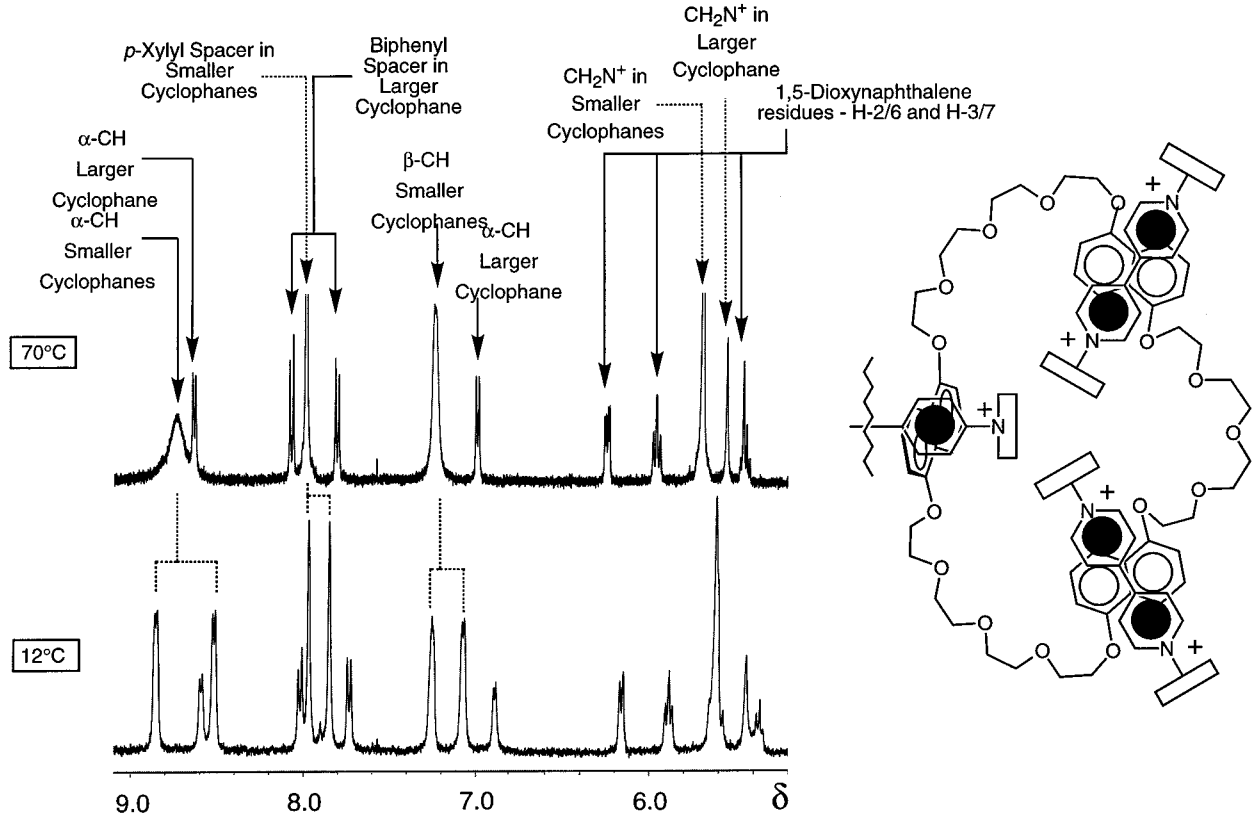

Figure 13. Partial ^{1}H NMR spectra of the [7]catenane **23**·20PF$_6$ at 285 and 343 K (400 MHz, CD_3CN).

processes should be observed. We have examined the electrochemical behavior of [2]catenane **13**$^{4+}$, [3]catenane **14**$^{8+}$, [2]catenane **17**$^{4+}$, [3]catenane **18**$^{4+}$, [5]catenane **20**$^{12+}$ (Olympiadane), and [7]catenane **23**$^{20+}$.

Table 3. Electrochemical Properties of the Examined Catenanes and Their Components[a]

compd	E_{red} [n] (ΔE)	E_{ox}[b,c]
TN57C15		+0.98; +1.15; +1.25
24^{4+}	−0.28 [2.0] (62); −0.72 [2.0] (65)	
25^{4+}	−0.31 [1.9] (67); −0.72 [1.9] (66)	
13^{4+}	−0.36 [1.1] (68); −0.47 [0.9] (63); −0.81 [1.6] (81)	+1.19; +1.26; +1.57
14^{8+}	−0.33 [1.9] (72); −0.41 [1.9] (68); −0.79 [1.8] (64); −0.85 [1.8] (60)	+1.31; +1.60
17^{4+}	−0.30 [0.9] (82); −0.39 [1.0] (83); −0.73 [1.8] (65)	+1.16; +1.26; +1.52
18^{4+}	−0.45 [1.9] (92); −0.82 [2.0] (65)	+1.07; +1.12; +1.23; +1.51
20^{12+}	−0.34 [2.0];[c,d] −0.39 [3.7];[c,d] −0.84 [5.9] (80)	+1.14; +1.34; +1.41; +1.56
23^{20+}	−0.29 [5.4];[c,e] −0.37 [4.6];[c,e] −0.87 [9.5][c,e]	*f*

[a] Argon-purged MeCN solution, 298 K; halfwave potential values in V vs SCE; reversible processes, unless otherwise noted; for reversible processes, [n] = number of exchanged electrons, (ΔE) = separation in mV between cathodic and anodic peaks in cyclic voltammograms. [b] All oxidation processes are not fully reversible. [c] Potential values estimated from DPV peaks. [d] Not resolved with CV technique. [e] The anodic part of the cyclic voltammogram is affected by adsorption phenomena. [f] No oxidation process has been observed.

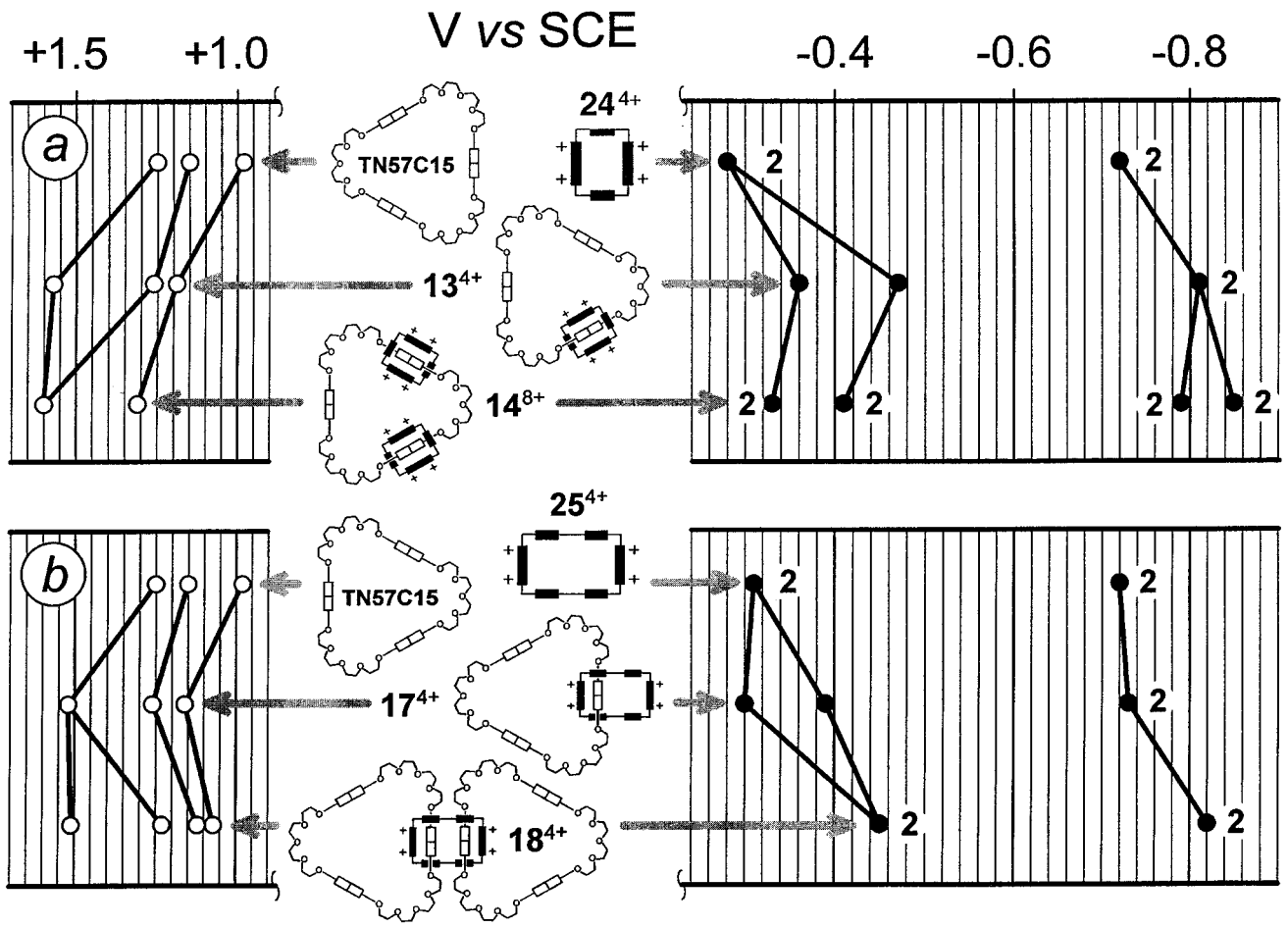

Figure 14. Correlation diagrams for the electrochemical behavior: (a) [2]catenane **13**$^{4+}$, [3]catenane **14**$^{8+}$, and their **24**$^{4+}$ and **TN57C15** components; (b) [2]catenane **17**$^{4+}$, [3]catenane **18**$^{4+}$, and their **25**$^{4+}$ and **TN57C15** components.

B. [2]Catenane 13^{4+} and [3]Catenane 14^{8+}. The correlation diagram for [2]catenane **13**$^{4+}$, [3]catenane **14**$^{8+}$, and their components **24**$^{4+}$ and **TN57C15** is shown in Figure 14a. In the catenanes, the two electroactive units of **24**$^{4+}$ are engaged in donor−acceptor interactions and occupy spatially different sites. Therefore, it can be expected that their reduction takes place in separated processes at more negative potentials compared to free **24**$^{4+}$. This is clearly the case for the first reduction of the two bipyridinium units in **13**$^{4+}$: the "alongside" unit is reduced at −0.36 V, and the "inside" one at −0.47 V. Comparison with the previously investigated [2]catenane,[19] composed of **24**$^{4+}$ and **DN38C10**, shows that in **13**$^{4+}$ the first reduction process occurs at a slightly more negative potential, whereas the second one is considerably displaced toward less negative potentials. This difference could result from the great flexibility of the **TN57C15** macrocycle which (i) allows one of the **DMN**-type units to interact with the "alongside" bipyridinium unit of the cyclophane and, at the same time, (ii) does not force two **DMN**-type units to sandwich the "inside" bipyridinium unit. After the first reduction, the electron donor−acceptor interaction becomes weaker and the flexible nature of the **TN57C15** macrocycle could facilitate a fast interchange between monoreduced "inside" and "alongside" units, with a consequent lack of splitting of the second process. For [3]catenane **14**$^{8+}$—composed of **TN57C15** and two equivalent **24**$^{4+}$ cyclophanes—(Figure 15), simultaneous reduction of the "alongside" units of the two cyclophanes is followed by simultaneous reduction of the "inside" units. Both processes are displaced to less negative potentials compared with **13**$^{4+}$ because the ratio between electron−donor and electron−

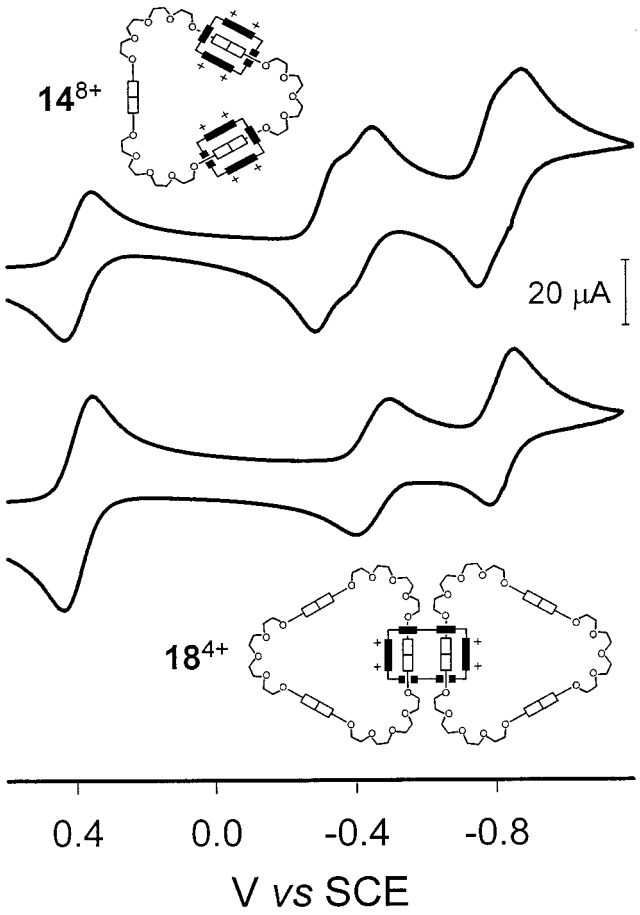

Figure 15. Cyclic voltammograms for reduction of [3]catenanes $\mathbf{14}^{8+}$ and $\mathbf{18}^{4+}$ (MeCN solution, 298 K, scan rate 200 mV s^{-1}, glassy carbon as working electrode). The wave with $E_{1/2} = +0.40$ V is that of ferrocene used as a standard.

acceptor units decreases from 3/2 to 3/4. The splitting of the second reduction process of the bipyridinium units is consistent with the crowded structure of the catenane, which presumably prevents fast interchange between "inside" and "alongside" units.

In $\mathbf{13}^{4+}$, the three **DMN**-type units of the **TN57C15** macrocycle undergo distinct oxidation processes. As a consequence of the charge-transfer interaction, all these processes move to more positive potential values with respect to the free macrocycle. A detailed comparison between the two oxidation patterns is made difficult because, in the catenane structure, the donor−acceptor interactions between non-oxidized and oxidized **DMN**-type units are partially or completely prevented. In the [3]catenane $\mathbf{14}^{8+}$, only two oxidation processes are observed, a feature that is consistent with the presence of an "outside" and two equivalent "inside" **DMN**-type units.

C. [2]Catenane $\mathbf{17}^{4+}$ and [3]Catenane $\mathbf{18}^{4+}$. The correlation diagram for $\mathbf{17}^{4+}$, $\mathbf{18}^{4+}$, and their components, $\mathbf{25}^{4+}$ and **TN57C15**, is shown in Figure 14b. On reduction, a general displacement toward more negative potentials is observed on going from the free cyclophane $\mathbf{25}^{4+}$ to its catenanes. In $\mathbf{17}^{4+}$, the first reduction of the two bipyridinium units of the cyclophane component occurs, as expected, in two distinct processes. It is worth noting that the first process is not at all diplaced, indicating that the "alongside" unit is practically unperturbed by the macrocyclic polyether. This situation is presumably related to the large size and rigidity of the cyclophane, which, in the most stable catenane geometry, leaves one of the two bipyridinium units far away from the electron-donor units of **TN57C15**. The lack of splitting of the second process, already observed for $\mathbf{13}^{4+}$, and its very small displacement toward more negative potentials clearly indicate that, once the two bipyridinium units have been monoreduced, the large size of the two components prevents any further charge-transfer interaction. The oxidation pattern of $\mathbf{17}^{4+}$ is fully consistent with that observed for $\mathbf{13}^{4+}$.

The [3]catenane $\mathbf{18}^{4+}$ shows two bielectronic reduction processes, because the two bipyridinium units of $\mathbf{25}^{4+}$ occupy equivalent positions. Figure 15 shows the cyclic voltammogram for the reduction of $\mathbf{18}^{4+}$. The strong displacement toward more negative potentials, compared with $\mathbf{25}^{4+}$, is obviously due to the charge-transfer interaction with the electron-donor units of the encircling macrocyclic polyether. The further displacement, compared to that observed for the first reduction of the "inside" unit of $\mathbf{17}^{4+}$, can be attributed to the presence of two **DMN**-type units inside the cyclophane. This feature could favor a geometry where a close approach between the electron-donor and -acceptor units is sterically enforced, thereby optimizing the charge-transfer interaction. As indicated by the noticeable displacement of the second reduction to more negative potentials, such a structure seems to be essentially maintained, even after one-electron reduction of the two bipyridinium units. In conclusion, the reduction pattern of $\mathbf{18}^{4+}$ is consistent with a structure like that shown in Figure 4. The oxidation pattern (Figure 14b), although very complicated, is consistent, at least from a qualitative viewpoint, with a structure of the type shown in Figure 4. The first process is assigned to the oxidation of the two **DMN**-type units not involved in stacking interactions, the second one to the two "alongside" units, and the subsequent ones to oxidation of the two (interacting) **DMN**-type units contained inside the cyclophane.

D. [5]Catenane $\mathbf{20}^{12+}$ (Olympiadane) and [7]Catenane $\mathbf{23}^{20+}$. These multiply interlocked catenanes contain a large number of electroactive units: six **DMN**-type units and six bipyridinium units in Olympiadane, and six **DMN**-type units and 10 bipyridinium units in $\mathbf{23}^{20+}$. It is worth noting that *no oxidation process* has been observed for $\mathbf{23}^{20+}$. Oxidation of $\mathbf{20}^{12+}$ shows a pattern consistent with its structure: a process attributed to the two **DMN**-type units not encircled by cyclophanes is followed by a second process assigned to oxidation of the two **DMN**-type units encircled by smaller cyclophanes. The two subsequent processes can be assigned to oxidation of the interacting **DMN**-type units inside the larger cyclophane.

For Olympiadane ($\mathbf{20}^{12+}$), the first two-electron reduction process can be assigned to simultaneous one-electron reduction of two "alongside" bipyridinium units of the smaller cyclophanes. The subsequent four-electron process can be attributed to the simultaneous reduction of two "inside" bipyridinium units of the smaller cyclophanes, which overlaps with the reduction process of the two equivalent bipyridinium units of the larger cyclophane. These results are consistent with the structure shown in Figure 7, where two bipyridinium units of the $\mathbf{24}^{4+}$ cyclophanes are at least partially engaged with two nonencircled **DMN**-type units of the two **TN57C15** macrocycles. The second reductions of all six bipyridinium units overlap, giving rise to a broad DPV peak at −0.84 V.

On reduction, $\mathbf{23}^{20+}$ yields two processes characterized by two large DPV peaks. Each process corresponds to the exchange of 10 electrons, as expected for the first and second reduction of the ten bipyridinium units of the five cyclophanes. The first DPV peak shows a shoulder and can be analyzed as made of two overlapping peaks whose areas are in a ratio close to 6:4. The first component peak is much larger than the second

one, suggesting that in its turn it results from overlapping processes. Second reductions of all the bipyridinium units merge into a broad DPV peak at −0.87 V.

Concluding Remarks

The results that we have presented and discussed in this paper lead us to draw the following conclusions:

(a) The best synthetic approach so far to higher catenanes, based on ring components with matching π-electron donating and π-electron accepting units, involves a two-stage procedure whereby a [3]catenane is self-assembled first of all in one step, and then, subsequently, in further successive steps—namely one through four—it is converted into one [4]catenane, two isomeric [5]catenanes, one linear and one branched, and one [6]catenane and one [7]catenane, both branched.

(b) In the self-assembly of higher order catenanes, i.e., those involving more than three interlocked rings, which result from the template-directed formation of tetracationic cyclophanes containing two π-accepting bipyridinium units on a repetitive basis around suitably sized crown ethers comprised of two or more π-donating recognition sites, the 1,5-dioxynaphthalene ring system provides a much better template than does the hydroquinone ring.

(c) Although ultrahigh pressure reaction conditions proved beneficial subsequently in driving the kinetically controlled self-assembly process involving the template-directed formation in a stepwise manner of cyclobis(paraquat-*p*-phenylene) tetracations around the remaining four "free" 1,5-dioxynaphthalene recognition sites in the intermediate [3]catenane to afford catenanes with four through seven rings, it was not helpful in the process of self-assembling this key intermediate in the first place.

(d) In the solid state, both the [3]- and the [5]catenane exist as centrosymmetric molecules that manage to maximize the use of many different kinds of noncovalent bonding interactions between matching donor and acceptor units in the components. Although the [7]catenane does not feature a center of symmetry, a total of four highly ordered hexafluorophosphate counterions are located symmetrically in pairs in two different voids in the molecular structure of this polycation carrying 20 positive charges. Perhaps the anions actually assist in the self-assembly process, leading first to the [6]catenane and then to the [7]catenane.

(e) Dynamic ^{1}H NMR spectroscopy of the catenanes in solution reveals that the rates of circumrotation of the rings with respect to each other varies markedly on going from the lower to higher order catenanes. One thing is sure in systems where the changes in co-conformations are extremely complex—the circumrotation of the crown ether rings through the tetracationic cyclophane becomes more and more difficult on progressing from the lower to the higher order catenanes.

(f) In the lower order catenanes, the electrochemical processes can be assigned to specific units. In the higher order catenanes, where a large number of electrons are exchanged, overlap of processes makes difficult specific assignments, but the overall picture is consistent with their molecular structures.

In summary, our research has demonstrated that a synthetic methodology, which affords [2]catenanes in excellent yields, can be extended, in principle at least, as far as a branched [7]-catenane. The question is the following: Where do we go from here? Of many possible approaches to polycatenanes, two that appeal to us currently involve (1) the linking together of oligocatenanes (two [6]catenanes to give, for example, a [13]-catenane) and (2) the use of a more traditional synthetic approach to fuse together covalently some [2]catenane "monomers", followed by subsequent rearrangements or chemical modifications to afford oligocatenanes and ultimately polycatenanes. One thing is certain: it is only a matter of time now until the making of polycatenanes will be a routine activity in the research laboratory.

Acknowledgment. This research was supported by the British Council, the Biotechnology and Biological Sciences Research Council, and the Engineering and Physical Sciences Research Council in the UK. Financial support from the Italian MURST and University of Bologna (Funds for Special Projects) is also acknowledged. This work has been carried out within the framework of the EU TMR Project FMRX-CT96-0076.

Supporting Information Available: Experimental procedures and tables of cystallographic data (44 pages, print/PDF). See any current masthead page for ordering information and Web access instructions.

JA9720873